Surface Immobilized Nucleic Acid–Transcription Factor Quantum Dots for Biosensing

Mingfu Chen, Thuy Nguyen, Nitinun Varongchayakul, Chloé Grazon, Margaret Chern, R. C. Baer, Sébastien Lecommandoux, Catherine Klapperich, James E Galagan, Allison M. Dennis, et al.

Author manuscript of article published in *Adv. Healthcare Mater. 2020*

Surface Immobilized Nucleic Acid - Transcription Factor Quantum Dots for Biosensing

Mingfu Chen,[1] Thuy T. Nguyen,[1] Nitinun Varongchayakul,[1] Chloé Grazon,[2,3] Margaret Chern,[1] R C. Baer,[4] Sébastien Lecommandoux,[3] Catherine M. Klapperich,[1,5*] James E. Galagan,[1,4*] Allison M. Dennis,[1,5*] and Mark W. Grinstaff [1,2,5*]

Received March 12 2020, accepted online July 21 2020

doi.org/10.1002/adhm.202000403

1 Department of Biomedical Engineering, Boston University, Boston, MA 02215, USA
2 Department of Chemistry, Boston University, Boston, MA 02215, USA
3 CNRS, Bordeaux INP, LCPO, UMR 5629, Univ. Bordeaux, F-33600, Pessac, France
4 Department of Microbiology, Boston University, Boston, MA 02118, USA
5 Division of Materials Science and Engineering, Boston University, Boston, MA 02215, USA

Keywords: biosensing, transcription factor, quantum dots, Förster resonance energy transfer

Abstract: Immobilization of biosensors on surfaces is a key step towards development of devices for real world applications. Here we describe the preparation, characterization, and evaluation of a surface bound transcription factor – nucleic acid complex for analyte detection as an alternative to conventional systems employing aptamers or antibodies. The sensor consists of a gold surface modified with thiolated Cy5 fluorophore-labeled DNA and an allosteric transcription factor (TetR) linked to a quantum dot. Upon addition of anhydrotetracycline (aTc) – the analyte – the TetR-QDs release from the surface-bound DNA, resulting in loss of the Förster resonance energy transfer (FRET) signal. The sensor responds in a dose-dependent manner over the relevant range of 0-200 μM aTc with a limit of detection of 80 nM. The fabrication of the sensor and the subsequent real-time quantitative measurements establish a framework for the design of future surface-bound, affinity-based biosensors using allosteric transcription factors for molecular recognition.

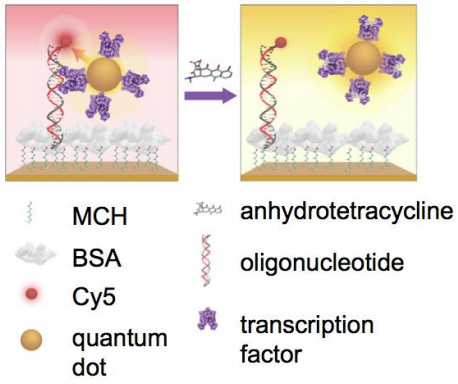

M. Chen,T. T. Nguyen, N. Varongchayakul, C. Grazon, M. Chern, R C. Baer, S. Lecommandoux, C. M. Klapperich, J. E. Galagan, A. M. Dennis, M.W. Grinstaff Adv. Healthcare Mater. 2020 doi.org/10.1002/adhm.202000403

1. Introduction

Biosensors are advancing medical practice and catalyzing the consumer market with new products.[1] Two key requirements for continued growth and development of this technology revolution are the identification of new sensing elements for analytes of interest and the immobilization of the sensing element to afford a surface-based readout.[2] With regards to the former, the sensor elements commonly used are based on antibodies, aptamers, and enzymes, and employ a change in an optical or electrical signal upon analyte recognition.[3] Transcription factors, mined from bacteria, are recently reported as new signal transduction elements when integrated with a quantum dot-based Förster resonance energy transfer (QD-based FRET) read-out.[4] This finding opens the door to a class of new sensors for detecting almost any small molecule, as bacteria sense and respond to a large number of compounds.[2b] Given that the biological function of transcription factors involves binding to double-stranded DNA, a mechanism for surface immobilization via the DNA is naturally integrated or pre-installed within the sensor element, as immobilizing DNA on a surface is widely used for a number of applications (e.g., gene chips,[5] environmental monitoring,[6] and food safety testing[7]).

Tetracyclines are extensively prescribed as broad-spectrum antibiotics to prevent and treat bacterial infections due to their effectiveness, low cost, and safety profile.[8] Global antibiotic consumption in humans and livestock is estimated to be more than 60,000 tons per year. However, the increasing rate of bacterial resistance as well as the excretion of significant quantities of tetracycline after *in vivo* administration due to limited metabolic degradation warrants monitoring from both health and environmental perspectives.[9] Classical quantitative methods for tetracycline concentration determination include photometry,[10] HPLC with mass spectrometry,[11] UV detection,[12] and enzyme immunoassay.[13] While useful, the disadvantages of complexity, low sensitivity, and high cost of analysis are spurring the development of new detection strategies such as aptamer based photoelectrochemical[14] and nanoparticle based fluorescent sensors.[15]

Within the tetracycline family, the derivative anhydrotetracycline (aTc) binds a known bacterial transcription factor and is an ideal model system for development of a surface immobilized sensor based on allosteric transcription factor (aTF)-DNA binding.[16] Regulatory aTF proteins comprise a ligand-binding domain as well as a DNA-binding domain. Upon ligand binding, aTFs undergo a conformational change that alters their affinity for an operator DNA sequence.[17] To generate an optical readout of the aTF-DNA binding, which decreases upon addition of the aTF effector molecule, (i.e., our analyte), we will use Förster resonance energy transfer (FRET) between a quantum dot (QD) attached to the protein and a dye-labeled DNA. Specifically, the QD-FRET sensor consists of 1) a polyhistidine-tagged Tet repressor (TetR) self-assembled on a CdSe/CdS/ZnS core/shell/shell QD bound and 2) its cognate DNA sequence immobilized on gold through a thiolated linker and hybridized with a Cy5-labeled complementary strand (**Figure 1**). TetR detaches from the DNA in a dose-dependent response manner to aTc, inducing a change in FRET signal (Figure 1c and 1d). Herein we report the: 1) preparation of TetR-labeled CdSe/CdS/ZnS QDs and DNA-functionalized surface; 2) immobilization of the TetR-QD conjugate to the surface; 3) importance of surface passivation on sensor performance; 4) AFM

characterization of the surface assembled sensors; 5) calibration curve of FRET emission versus aTc concentration along with the measured limit of detection (LOD); and, 6) design guidelines for engineering an optimized surface bound transcription factor-based biosensor.

2. Results and Discussion

Solution-phase optical sensors are of significant use, however adaptation of the design for analyte detection on a surface expands the potential application space (e.g., DNA microarrays,[18] point-of-care (POC) diagnostics,[19] and chemical sensors[20]). Additionally, such sensors can be incorporated into lateral flow or microfluidic devices for facile sample preparation and liquid handling as well as integrated into devices for multiplex detection with other sensors. As a first step towards such devices, we recognize that our QD-FRET sensor based on a QD grafted with a transcription factor and a fluorophore-labeled nucleic acid duplex is amenable for surface immobilization given the precedent for linking DNA to varied surfaces including gold[21], silica substrate[22], and carbonaceous materials[23]. The alternative design whereby the transcription factor grafted QD is linked to the surface is less attractive because multistep synthetic schemes would be required to immobilize the QD[24] and immobilization of proteins often leads to loss of function and denaturation. In the forthcoming text, we first describe the synthesis and characterization of the sensor parts – QD, transcription factor, and DNA – followed by sensor construction and performance evaluation. Finally, we discuss this surface-immobilized QD system with respect to transcription factor-based biosensors previously reported in the literature.

2.1. QD Synthesis and Characterization. We synthesized CdSe/CdS/ZnS QDs through a layer-by-layer shelling strategy,[25] targeting an emission maximum of 620 nm for the core/shell/shell CdSe/CdS/ZnS QDs in order to generate efficient QD→Cy5 FRET. Briefly stated, Cd cations chelated by oleic acid were dissolved in octadecene and heated to high temperature (**Figure 2**a). A mixture of trioctylphosphine selenide (TOP:Se) and long-chain amines were rapidly injected into the hot Cd solution, nucleating CdSe nanoclusters. We then coated the CdSe cores with CdS and ZnS, using a successive ion layer adsorption and reaction (SILAR) process to impart a thick, epitaxial shell on the core.[25] Once synthesized, we transferred the QDs into water via a ligand exchange reaction using a dithiol anionic molecule 3-[(2-carboxyethyl)[2-(6,8- disulfanyloctanamido)ethyl]amino]propanoic acid (compact ligand 4, CL4)[26]; CL4 coatings are known to produce stable QDs in aqueous media and allow histidine-mediated self-assembly of proteins to the QD.[27] Self-assembly of the transcription factor TetR-His_6 onto the QD was driven by metal-affinity of the His-Tag.[28] The TetR functionalized QDs are spherical and on average 7.6 ± 1.1 nm in diameter by TEM (Figure 2b) and 10 ± 2 nm by DLS. QD excitation at 400 nm affords a photoluminescence (PL) emission spectrum with a λ_{max} at 620 nm and a QY of 23.4 ± 2.3 % (**Figure S1**).

2.2. Oligonucleotides immobilization and quantification. We derivatized gold coated surfaces (glass, or microplates) with a 30-mer single stranded nucleic acid modified with an alkane thiol at the 5' end (ssDNA#1) and 6-mercapto-1-hexanol (MCH; see SI for details and **Table S1)**. MCH was selected as the spacer thiol for its ability to: 1) block nonspecific adsorption to the surface; 2) dissolve in aqueous

solution; and, 3) avoid interference in the hybridization reaction to surface bound DNA as the six-carbon chain of MCH is the same length as the methylene group spacer in thiol-linked ssDNA (Figure 1).[29] We subsequently hybridized ssDNA#2 to the Au-bound strand, which possesses a Cy5 fluorophore at the 5'end for FRET with the QD (**Table S1;** extinction coefficient = 313,200 $L \cdot mole^{-1} \cdot cm^{-1}$, λ_{max} = 666 nm; absorption and emission (λ_{exc}= 590 nm) **Figure S2**). The resulting dsDNA binds the transcription factor with a K_D = 0.0830 nM.[28c]

To estimate the quantity and surface coverage of the dsDNA on the Au surface, we dehybridized Cy5-labeled complementary ssDNA#2 from the Au/MCH/Cy5-DNA surface and measured the concentration of ssDNA#2, via Cy5 fluorescence, using an established standard calibration curve (Figure S2). From this procedure, we found the density of DNA on the surface and surface coverage to positively correlate with the concentration of DNA in the overnight incubation buffer (**Figure S3**). The use of higher DNA concentrations yielded increased surface coverage. Based on this step, a concentration of 100 μM for both the thiolated DNA and its complementary strand was selected for all subsequent experiments.

2.3. Surface passivation and binding studies. We first tested the QD transduction of the probe system by measuring and then comparing the emission spectra of the surface probe system to its aqueous solution counterpart (**Figure 3**).[28c] In both cases, FRET occurs between a red-emitting QD and the fluorophore Cy5. Donor-acceptor spatial modulation is an established method to create a ratiometric response where QDs function as donors and a dye as the acceptor.[28c, 30] Herein, QD-based FRET occurs as the QD transcription factor binds to the Cy5-labeled oligonucleotide because the QD and fluorophore are in close proximity. While QDs possess many favorable optical properties, surface energy transfer is a potential concern when designing a surface immobilized QD transduction system.[31] The emission spectra of our surface probe system, Au/MCH/Cy5-DNA/BSA + (TetR-QD) is shown in Figure 3a. The QD emission is similar compared to the emission from its aqueous solution counterpart (Figure 3b). The FRET efficiency is higher (not statistically significantly) in the surface probe system (31.2% vs. 26.0%).

Next, we evaluated the effect of BSA passivation on the surface DNA-QD-TF system, as BSA is known to block non-specific binding, facilitating sequence-specific binding (Figure 1b).[32] Using the Cy5-DNA coated surface (Au/MCH/ Cy5-DNA), prepared as described above with 100 μM DNA **(**oligonucleotide # 1 and 2 in Table S1), the effect of different concentrations of BSA and incubation times were determined for DNA-QD-TF performance. Upon excitation at 400 nm, the emission at 620 nm was measured as an indicator of the amount of QDs (or QD-TFs) bound to the surface. Based upon our prior experience,[33] we selected two BSA concentrations, four BSA incubation times, and two QD-TetR incubation times to identify a condition to passivate the Cy5-DNA coated surface (Au/MCH/Cy-DNA) and minimize nonspecific adsorption. Following QD-TF incubation, samples were measured for QD emission intensity (**Figure S4**). The QD emission intensity was consistently higher with 30 min QD-TetR incubation times than 10 min incubation times. The highest QD intensities were seen for samples that were incubated with the QD-TetR for 30 mins and with BSA for only a short period of time (e.g., 10 min). Under these conditions, an increase in BSA concentration from 0.05% to 0.5% (w v^{-1}) moderately increased the QD intensity

(Figure S4b), likely due to the excess of nonspecific binding.[32] Although both BSA concentrations elicit a passivation effect over time, to minimize nonspecific binding, 0.05 wt% BSA passivation for 360 min and 0.18 μM QD-TF incubation for 10 min were used for all subsequent experiments.

Lastly, we quantified the binding of QD and QD-TF conjugates to various modified surfaces **(Figure 4)**. Upon passivation with 0.05 wt% BSA, most surfaces show decreased QD-TF binding compared to their counterparts without BSA treatment (Figure 4b). The surfaces with sequence specific DNA afford greater QD-TF binding compared to surface lacking DNA or coated with nonspecific DNA sequences (Figure 4c and d). These observations are in line with transcription factor recognition mediated by sequence specific DNA.

2.4. Nanotopology surface characterization. To visualize the modified gold surfaces, we characterized the samples using atomic force microscopy (AFM). We first imaged the gold surface treated with MCH and Cy5-DNA. The Au/MCH/Cy-5DNA surface is uniformly flat, similar to the bare gold surface (**Figure 5**a, additional data in **Figure S5**). The Au/MCH/Cy5-DNA's surface roughness, defined by the root-mean-square value of the height, is 1.47 nm, comparable to 1.49 nm for the bare gold. After BSA treatment and QD-TF incubation, the Au/MCH/Cy5-DNA/BSA + (TetR-QD) surface exhibits heterogeneous features, with an increased surface roughness of 3.23 nm (Figure 5b). Particle sizing analysis reveals multiple populations of the particles. The particles of 7.7 ± 0.8 nm and 9.9 ± 1.2 nm in diameter (marked as spot 1 and 3 in Figure 5b and c, respectively) correspond to the size of the BSA protein measured from crystal structure (Protein Data Bank file No. 3V03) (Figure 5d). Notably, there is an additional population of the particles with heights greater than 15 nm on the surface (marked as spot 2 in Figure 5b). We propose that these are QD-TF conjugates, as the value matches the expected size of the QD- TF conjugates. The relatively sparse distribution of QD-TF conjugates avoids possible crowding effect introduced by attachment of the QD-TF conjugates, which will alter the diffusion-limited reaction kinetics when later subjected to aTc solutions.

To further characterize the particles on the surface, we collected force curves, correlating cantilever tip indentation depth with force. Force spectra on the particles less than 15 nm show a saw-tooth pattern upon retraction, suggesting that they are soft protein species (Figure 5e).[34] Spot 1 is likely BSA. In contrast, the force spectra collected on the particles larger than 15 nm show no pulling curve upon retraction. This different force response suggests that the larger particles are solid quantum dots.[35] Spot 2 is likely QD- TF conjugate.

Lastly, we introduced the aTc solution onto the Au/MCH/Cy5-DNA/BSA + (TetR-QD) surface to dissociate TetR-QD from the surface. The surface roughness correspondingly changes and exhibits a roughness of 1.67 nm, similar to that of bare gold and Au/MCH/Cy5-DNA surface. No particles larger than 15 nm are found, indicating the absence of QDs on the surface. From these results, the QD-TF is successfully released from the surface upon treatment with aTc.

2.5. Dose response studies. We evaluated the analytical response of the surface probe system towards aTc by quantifying the QD-TF bound to the surface upon

exposure to 0 - 200 μм aTc in Tris Buffered Saline pH 7.4 (Figure 1c and d). We normalized the emission intensity at 620 nm to the emission intensity before aTc exposure, thus allowing an assessment of remaining QD-TF conjugates bound to the surface as a function of aTc concentration without the influence of sample preparation variance. The relative intensity of the surface probe system negatively correlates with treatment time and aTc concentration (**Figure 6**a). These observations are consistent with TetR's allosteric response to aTc: a profound decrease in its binding affinity to its operator DNA,[36] providing the mechanism behind the detection aTc.[37] In this study, aTc is recognized by TetR. However, we are cognizant of the recognition of other tetracycline-like antibiotics, such as lymecycline, minocycline,[38] and doxycycline,[39] by TetR due to its broad specificity. To address this, methods such as directed evolution have been applied to tailor TetR's specificity.[40]

The relative intensity decreases correlate with an increase in aTc concentration over the range of 0-200 μм at a response time of 32 min (Figure 6b). Here, the relative QD emission intensity represents the amount of QD-TFs bound to the surface (*i.e.,* higher relative intensity values indicate more aTF-DNA binding). Higher concentrations of aTc and longer treatment times favor the unbinding of QD-TF from its operator DNA (oligonucleotide # 1 and 2 in Table S1). The resulting surface has less QD-TF, which in turn lowers the emission intensity (**Figure S6**). These experiments are diffusion-limited, so the intensity depends on both the aTc concentration and the treatment time.

Next, we assessed the aTc sensor's performance over the range of 0-200 μм. The surface probe system displays a reproducible response (e.g., relative standard deviation = 5.9%, n=3, at 5 μм aTc), after a response time of 32 min (Figure 6b). The data of the relative intensity and aTc concentration are fit to a four-parameter logistic function. The limit of detection (LOD), defined as the aTc concentration, yields a signal greater than 3 times the pool standard deviations above background (i.e., 0.08 μм). The relatively short response time enables real-time quantitative determination of aTc in samples, with an IC_{50} of 3.4 μм. The coefficient of determination, a measurement of how well the four-parameter logistic regression approximates the data points, is 0.95 at a response time of 32 min. The sensor performances at different response times are summarized in **Table S2**. Interestingly, with a shorter response time, the IC_{50} of the surface probe system increases (Figure S6). For example, after a response time of 4 min, the IC_{50} increases to 91 μм. Such a time-dependent response offers a means to optimize the dynamic range of the sensor. For example, longer response time shifts the detection capability to the lower concentration range. This capability is not present in the solution assay Affinity-based sensors differ from solution-phase to surface-phase.[41] Different local environment for surface-phase binding, multivalent QD-TetR, and kinetics of DNA–TetR binding are the likely reasons that the surface probe system demonstrates time-dependent response, a phenomenon absent in the solution-phase FRET systems. Notably, these results emphasize the potential of modulating the affinity binding of transcription factor for its operator DNA to modify the performance of such sensing system. Reducing the affinity between TF and its operator DNA (or increasing the affinity between TF and target chemicals) is also one reported approach to lower the response time and limit of detection.[28c, 42] Additionally, it is worth noting that tuning the solution-based sensors' sensitivity can be achieved by changing aTF concentration: increasing the aTF concentration to desensitize the sensor (dose response shifts to higher concentrations), or decreasing the aTF concentration to

sensitize the sensor (dose response shifts to lower concentrations).[43] Further, a recent report describing a combined, aTF and DNA polymerase biosensor shows improved sensitivity through signal amplification.[44] While a biosensor based on aTF and CRISPR-Cas12a avoids the presence of aTF and Cas12a in the same solution, and thus minimizes the competitive binding to target, by immobilizing the aTF on cellulose.[45]

From a QD surface immobilization perspective, our system enables attachment of a nucleic acid - transcription factor quantum dots construct to a surface for biosensing. Such immobilized biosensors are of interest, as this is the first step towards development of an analyte detection device for real world applications.[46] Alternative approaches are described for QD immobilization including the use of a poly(acrylate) hydrogel.[47] QDs entrapped in this host hydrogel are protected from the bulk solution, and analytes must diffuse through the matrix to reach the QD. Another approach utilized QDs immobilized on silica optical fibers for nucleic acid detection.[48] In that case, the immobilization chemistry is based upon the thiol-metal affinity interaction between thiol ligands on fused silica surfaces and CdSe/ZnS quantum dots .[27a] Though effective, these methods require multistep synthetic schemes to immobilize QDs, and direct analyte oligonucleotide labeling is typically used. The surface immobilized biosensor, described herein, relies on the liquid/solid interfacial diffusion of analyte molecules. Separation of TF-DNA complex requires diffusive transport of the aTc to the complex resulting in separation of the QD-TF from the DNA. Our system combines the innate capability of biological and nanoparticle components, extending the merits of previous solid phase assays. However, several limitations or areas of improvement exist to include: 1) reduced reaction kinetics due to interfacial diffusion compared to solution-based sensor; 2) a multi-step immobilization procedure to construct the device; 3) detection is recorded as a loss of signal (i.e., off-sensor); and 4) a single use device. Transformation of this device to a reusable one will require design changes and further experiments, for example, entrapment of the sensor in a semi-permeable membrane which retains the QD but not the analyte. Importantly, our design and findings do complement the existing transcription factor-based sensors' transduction methods, with a quantum dot-based Förster resonance energy transfer read-out.

From a biology perspective, transcription factor based biosensor represents a next generation transduction strategy for sensor design with unique parameters and configurations for performance optimization.[4] In the current study, we present an *in vitro* transcription factor based sensor which utilizes a bacterial allosteric transcription factor. TetR's allosteric response to aTc decreases its binding affinity to its operator DNA, and was selected for this reason. Not all aTF decrease affinity upon binding an analyte. Previously, TFs have been widely used as *in vivo* whole-cell sensors (*i.e.,* the bacteria itself is the biosensor). Whole cell biosensors, however, are limited by slow response times, biosafety concerns, and the practical limitations of using a cellular host.[49] Only recently has a luminescent based solution phase assay been reported for measuring aTF-DNA binding activities for transducing analyte recognition into quantitative measurements.[42, 50] An additional advantage of this TF-DNA biosensor is the opportunity to alter (decrease or increase) the binding affinity using tools such as directed evolution.

3. Conclusion

We report surface-immobilized biosensors based on TF binding to DNA. The sensor consists of a transcription factor (TetR) linked to a core/shell quantum dot (CdSe/CdS/ZnS QD) and a gold surface with thiolated Cy5 fluorophore labeled DNA. Upon analyte (anhydrotetracycline) addition, the TetR-QD conjugates are released from the surface, resulting in a loss of signal. The key elements of this sensor include: 1) DNA with specific sequence to mediate TF recognition; 2) BSA to minimize nonspecific adsorption; 3) TF to bind to the surface by recognizing DNA sequence; and, 4) QD bound transcription factors as new signal transduction elements. The surface probe system enables real-time quantitative determination of aTc in samples. In summary, this surface immobilized sensing system using QD-TF as the transduction element holds promise for novel biosensor development by leveraging the engineering capabilities of the affinity binding and the versatility of transcription factor recognition.

4. Experimental Section

Measurements: Microplate experiments were analyzed using a SpectraMax M4 Multi-Mode Microplate Reader (Molecular Devices, LLC, CA). Atomic force microscopy experiments were analyzed using Molecular Force Probe 3D Instrument (MFP-3D, Asylum Research, CA). Average hydrodynamic diameters of nanoparticles were obtained using dynamic light scattering (DLS) on Brookhaven 90plus Nano-particle Sizer (Brookhaven Instruments Corporation, NY) at 25°C. Fluorescence spectra were measured at Nanolog spectrofluorometer (HORIBA, Ltd., NJ). Intensity is measured in relative fluorescence units, when excited at 400 nm (λ_{exc}= 400 nm), with baseline correction according to manufacturer's instruction. Transmission electron microscopy (TEM) images were acquired using a JEOL 1200EX (JEOL USA, Inc., MA) operating at an accelerating voltage of 5.0 kV.

Materials: Phosphate buffered saline (PBS) was purchased from Life Technologies (Grand Island, NY). Trioctylphosphine oxide, octadecene, cadmium oxide, oleic acid, oleylamine, hexanes, methanol, ethanol, trioctylphosphine, selenium, zinc acetate, 6-mercapto-1-hexanol (MCH), glycerol, anhydrotetracycline (aTc), bovine serum albumin (lyophilized powder, ≥96%), tris(hydroxymethyl)aminomethane, and Amicon® Ultra Centrifugal Filters were purchased from Sigma-Aldrich (St. Louis, MO). Sulfur, Tris buffered saline (1X TBS, pH 7.4), Invitrogen™ UltraPure™ Salmon Sperm DNA Solution, Pierce Micro BCA Protein Assay kit, HisPur™ Ni-NTA Resin, and BioGold™ Microarray Slides were purchased from Fisher Scientific (Pittsburgh, PA). Gold coated Corning™ microplates were purchased from Nirmidas Biotech, Inc. (Palo Alto, CA). Oligonucleotides were purchased from Integrated DNA Technologies, Inc. (Coralville, IA) and were HPLC purified by the manufacturer. Lysozyme, Egg White was purchased from Gold Biotechnology, Inc. (St. Louis, MO). Cantilevers were purchased from Bruker Nano Inc. (Camarillo, CA).

Transcription factor preparation: TetR-6His (TetR with 6x His-tags) was recombinantly produced with polyhistidine tags through *Escherichia coli*. Plasmids containing the gene for TetR were obtained through collaborative exchange (REF Dennis paper here). Plasmids were chemically transformed into *E. coli* BL21 with induction of lysogeny broth cultures at OD_{600} (optical density at 600 nm) values of 0.4 to 0.6 using 1мм isopropyl b-D-1-thiogalactopyranoside before analysis by SDS-

polysaccharide gel electrophoresis. Confirmed expression prompted 1-liter-scale cultures for expression and protein purification through disruption of cells using lysozyme and by passing cell lysate over a HisPur™ Ni-NTA Resin-packed column. Final protein products were quantified using the Pierce Micro BCA Protein Assay kit.

Synthesis and characterization of QD-TF conjugates: Quantum dot-transcription factor (QD-TF) conjugates were synthesized using the following three-step procedure.

First, QDs (CdSe/CdS/ZnS) were synthesized. CdSe cores were nucleated using a modified previous protocol.[51] Trioctylphosphine oxide (1g), octadecene (8 mL), and cadmium oleate (1.9 mL 0.2 M) were added to a 100 mL round bottom flask and degassed at room temperature for 30 min. The flask was then heated to 80°C and allowed to degas for another 30 min. The temperature was raised to 300°C and a pre-mixed solution of trioctylphosphine: Selenium (0.4 mL 1 M), oleylamine (3 mL), and octadecene (1 mL) was injected into the flask. After 3 min, the flask was removed from heat and allowed to cool to room temperature. To remove excess reagents and ligands, the raw QD core solution was pumped into a glovebox and precipitated out of solution using a mixture of methanol and ethanol. The cleaned CdSe cores were suspended in hexanes and stored at 4°C under air-free conditions for future use. Six CdS shell layers were added on top of the CdSe cores using a successive ion layer adsorption and reaction (SILAR) method.[52] Specifically, octadecene (5 mL) and oleylamine (5 mL) were added to a 100 mL round bottom flask and degassed for 30 min at room temperature and for an additional 30 min at 80°C. CdSe cores (200 nmol) in hexanes were injected in the reaction flask and allowed to degas for another 30 min at 80°C. Cadmium oleate was prepared from cadmium oxide and oleic acid. Zinc oleate was prepared from zinc acetate and oleic acid.[25] The cadmium oleate and sulfur injections were allowed to anneal for 2.5 and 1 hrs, respectively. The first cadmium oleate injection was done at 160°C and allowed to react for the 1 hour before increasing the temperature to 240°C for the remaining 1.5 hrs. The rest of the cadmium oleate and sulfur injections were performed at 240°C. An additional two layers of ZnS was added on top of the QDs to passivate the surface in preparation of water solubilization. The same SILAR method was used as above, except that 1 hour annealing times for the zinc oleate and sulfur precursors was used. CdSe/CdS/ZnS QDs were precipitated out of solution to remove any excess reagents using methanol and ethanol.

Second, QDs were transferred to water using a zwitterionic ligand that binds datively to the QD surface via a bidentate thiol linkage (compact ligand 4, CL4).[53] Specifically, QDs were dissolved in chloroform, mixed with the CL4 solution at a ratio of ~1200 CL4 molecules per unit surface area (nm^2), and stirred vigorously at room temperate overnight. CL4-coated QDs were purified using Amicon® Ultra Centrifugal Filters (Molecular weight cut-off: 30kDa). The excitation and emission spectra of QDs were measured by Nanolog spectrofluorometer.

Third, CL4-coated QDs were then reacted with TetR-6His at a 1:4 molar ratio for self-assembly of the TetR onto the QD surface at 22°C for 10 min in TBS with 5 mM $MgCl_2$, 5% glycerol, and 50 mg L^{-1} Invitrogen™ UltraPure™ Salmon Sperm DNA.

Diameter of QDs (CdSe/CdS/ZnS) was determined with TEM images analysis. Average hydrodynamic diameters of nanoparticles after ligand transfer with CL4 were

obtained using dynamic light scattering (DLS) on Brookhaven 90plus Nano-particle Sizer (Brookhaven Instruments Corporation, NY) at 25°C. The run time for each measurement was set for 1 min. Number weighted average is reported using particle refractive index of 1.6.

Preparation of QD-based FRET system: As a counterpart of surface probe system, QD-based FRET system was prepared by histidine-mediated self-assembly of proteins to the QDs in aqueous solution at a molar ratio of QD/TF/DNA of 1/4/18. QDs were mixed with TetR-His_6 at room temperature for 1hr. The double-stranded DNA (oligonucleotide # 6 and 7 in **Table S1)** labelled with Cy5 at the 3' and 5' ends was added to the mixture for 30 min incubation before diluted with TBS with 5 mM $MgCl_2$, 5% glycerol, and 50 mg L^{-1} Invitrogen™ UltraPure™ Salmon Sperm DNA. The excitation spectra of QD, QD/TF, and QD/TF/DNA were determined with Nanolog spectrofluorometer. FRET efficiency is calculated using the following expression: $E_{FRET}=1-F_{DA}/F_D$, where F_D is the emission intensity of the donor alone, and F_{DA} is the emission intensity of the donor in the presence of acceptor.[54]

Oligonucleotides immobilization and quantitation: Immobilization of 5' thiol-linked single-strand(ss) DNA onto gold coated surfaces (glass, or microplates) was performed by using the method previously described by Grinstaff and co-workers.[33] Specifically, various concentrations of the 5' thiol-linked ssDNA in 1 M potassium phosphate buffer was deposited onto the gold surface and left overnight. Two type of gold surfaces were used: BioGold™ Microarray Slides are gold coated glass surface; Nirmidas's gold coated microplates are based on polystyrene Corning™ 96-well plate. The gold surface was rinsed with Nanopure water after the removal of DNA solution. The gold surface was then exposed to 1 mM aqueous solution of 6-mercapto-1-hexanol (MCH) for 1 hr. To hybridize the immobilized ssDNA, the gold surface was exposed to solution of its complementary strand in 250 mM NaCl solution for 2 hrs before rinsed with 250 mM NaCl solution. To assess the surface coverage of the gold surface, surface density of DNA was measured using a fluorescence-based method described by Mirkin and co-workers.[55] Specifically, the complementary strand (oligonucleotide # 2 in **Table S1)** was labeled with fluorophore. The excitation and emission spectra of ssDNA#2 was determined with Nanolog spectrofluorometer. Dehybridization was performed by immersion of gold-covered glass surface in PBS at 95°C for 5 min before supernatant was taken out. Concentration of fluorophore and corresponding surface density of hybridized complementary strand was determined with SpectraMax M4 Multi-Mode Microplate Reader. Standard curve was prepared with known concentration of oligonucleotide # 2 (**Table S1**) in PBS. Surface coverage was calculated using a method described by Tarlov and co-workers.[56] Respective surfaces are named by their modifier content. For example, hybridizing transcription factor recognizing sequence of oligonucleotides with Cy5-labled complementary strand (oligonucleotide # 1 and 2 in **Table S1**), with mercaptohexanol as filler rendered the surface 'Au/MCH/Cy5-DNA'. BioGold™'s gold-coated glass surfaces were used as a standard model substrate for oligonucleotides quantification because of defined surface area, and for AFM studies due to their compliance with atomic force microscopy's sample stage. Nirmidas's gold coated microplates were used for all other experiments for high throughput measurements.

BSA passivation, and QD-TF binding studies: To determine if the surface binding events were affected by BSA concentration, BSA treatment time, and QD-TF incubation time, DNA coated surfaces (Au/MCH/Cy5-DNA) were prepared as described above with 100 μM DNA. Prior to QD-TF conjugates incubation, bovine serum albumin (BSA) was used to passivate the surface. Briefly, Au/MCH/Cy5-DNA surface was immersed in BSA solution of two concentrations (0.5 and 0.05 wt%) in Tris Buffered Saline (TBS) for 10-360 min. The surface was then rinsed with TBS. Following a 10-30 min incubation of Au/MCH/Cy5-DNA/BSA with 0.18 μM QD-TF conjugates prepared as described, the newly formed Au/MCH/Cy5-DNA/BSA + (TetR-QD) surface was rinsed with TBS and dried with nitrogen. The fluorescence intensity of QD of Au/MCH/Cy5-DNA/BSA + (TetR-QD), excited at 400 nm, was measured with Nanolog spectrofluorometer. All data points resulted from three independently formulated surface samples measured five times. 0.05 wt% BSA passivation for 360 min and 0.18 μM QD-TF conjugates treatment for 10 min were used for all subsequent experiments.

QD, QD-TF binding studies: To measure the nonspecific binding of QD-TF conjugates to various modified surface, similar fluorescence intensity test was performed. The surfaces were treated with TF sequence specific DNA (oligonucleotide # 1 and 2 in **Table S1**), which binds to TetR, or sequence nonspecific DNA (N.S.-DNA, oligonucleotide # 4 and 5 in **Table S1**), with or without MCH, with or without BSA and QD or QD-TF conjugates. For example, Au/MCH/N.S.-DNA/BSA+(TetR-QD) was prepared with gold surface with 1) modification of 5' thiol-linked single-strand(ss) DNA (oligonucleotide # 4 in **Table S1**), which is sequence nonspecific, 2) MCH treatment for 1 hr as described above, 3) complementary strand (oligonucleotide # 5 in **Table S1**) hybridization to nonspecific sequence, 4) 0.05 wt% BSA passivation for 360 min, and 4) QD-TF conjugates treatment for 10 min as described above. After the modification of various surfaces, the fluorescence intensity of QD on Au/MCH/N.S.-DNA/BSA+(TetR-QD), excited at 400 nm, was measured with Nanolog spectrofluorometer.

Dose response of the surface probe system: Dose response of Au/MCH/Cy5-DNA/BSA +(TetR-QD) surface to aTc was determined by spectrofluorometer. Preparation of QD-TF conjugate coated surface was carried out as outlined above. Sequence specific DNAs (oligonucleotide # 1 and 2 in **Table S1**) served as the binding site of QD-TF conjugates to the surface. The surfaces were treated with aTc solution (75 μL, 0-200 μM). At predefined time-points, aTc solutions were withdrawn from the surface, and the surfaces were rinsed with TBS. The resulting surfaces were measured with Nanolog spectrofluorometer for the QD emission intensity to quantify the amount of QD-TF conjugates on the surface. The relative intensity of QD left on the surface was calculated by normalizing QD emission at 620 nm by initial intensity (t=0) for each well/plate.

Nanotopology surface characterization: The atomic force microscopy (AFM) images were taken using Molecular Force Probe 3D Instrument (MFP-3D, Asylum Research, CA). The QD-TF conjugate coated glass before and after treatment with 200 μM aTc overnight were prepared as outlined above. The samples were rewet in DI water prior the experiment. A rectangular silicon nitride tip on a soft cantilever (MCLT, Bruker, CA) was chosen to minimize the damage to the protein sample. The imaging was collected in tapping mode in water. The roughness was calculated from root-

mean-square variation of the height (in z-direction) over the area of 5x5 μm^2 on three different locations.

Sensor evaluation: The sensor outputs are fit to a four-parameter logistic function:

$S(c) = S_1 + (S_0 - S_1)/(1+10^{((LogEC_{50} - c)*h)})$

where S_0 is the intensity of the sensor signal with no analyte present, S_1 is the intensity of the sensor signal at saturating analyte concentration, c is the analyte concentration, EC_{50} is the concentration of analyte that gives half-maximal response, and h is the Hill slope.

The limit of detection (LOD) is defined as the analyte concentration yielding a signal greater than 3 times the pool standard deviations above background.

The linear range is defined as the range of analyte concentrations for which the biosensor response changes linearly with the concentration. The interval is determined between the bend points, where the slope of the response changes upon approaching the lower and upper plateau.[57]

Statistical Analysis: Baseline correction was performed on fluorescence spectra data according to manufacturer's instruction. Absorption and photoluminescence intensity were normalized in Figure S1 and S2. The data are presented as mean ± standard deviation. Unless otherwise indicated, data presented were generated from three independent experiments. Multivariance analysis was done using one-way ANOVA that was corrected using the Bartlett's variance test, and for multiple comparisons, the Bonferroni multiple-comparison test was used. Statistical analysis was performed using the GraphPad Prism software (version 7.0; GraphPad Software Inc.).

Supporting Information.

Supporting Information is available from the Wiley Online Library or from the author.

Acknowledgements

The authors recognize support and funding in part from NIH (U54EB015403, CK; CTSI 1KL2TR001411, AMD), DARPA (W911NF-16-C-0044, JG, MWG, CK, AMD), BU Kilachand (JG), BME distinguished fellowship (MC), BUnano Terrier Tank award (MC), Clare Booth Luce Graduate Fellowship (Margaret C), and Marie-Curie Fellowship from the European Union under the program H2020 (Grant 749973, CG).

Author Contributions

M. Chen and MWG conceptualized and designed the overall study. MC conducted all experiments and analyzed the data. CG, TN, and M. Chern assisted with QD preparation and RCB with the transcription factor. NV conducted AFM-related studies and analyzed the data. The manuscript was written by M. Chen and MWG with contributions from all authors. All authors have given approval to the final version of the manuscript.

Conflict of Interest

A patent application has been filed with the US Patent Office and is available for licensing via Boston University.

References

[1] a) A. Tricoli, N. Nasiri, S. De, *Advanced Functional Materials* **2017**, *27*, 1605271; b) G. Appelboom, E. Camacho, M. E. Abraham, S. S. Bruce, E. L. Dumont, B. E. Zacharia, R. D'Amico, J. Slomian, J. Y. Reginster, O. Bruyère, E. S. Connolly, Jr., *Arch Public Health* **2014**, *72*, 28; c) D. Dias, J. Paulo Silva Cunha, *Sensors (Basel, Switzerland)* **2018**, *18*, 2414; d) A. K. Yetisen, J. L. Martinez-Hurtado, B. Ünal, A. Khademhosseini, H. Butt, *Advanced Materials* **2018**, *30*, 1706910.
[2] a) J. P. Chambers, B. P. Arulanandam, L. L. Matta, A. Weis, J. J. Valdes, *Curr. Issues Mol. Biol.* **2008**, *10*, 1; b) V. Libis, B. Delépine, J.-L. Faulon, *Current Opinion in Microbiology* **2016**, *33*, 105.
[3] a) A. J. Bandodkar, I. Jeerapan, J. Wang, *ACS Sensors* **2016**, *1*, 464; b) A. J. Bandodkar, J. Wang, *Trends in Biotechnology* **2014**, *32*, 363.
[4] C. Grazon, R. C. Baer, U. Kuzmanović, T. Nguyen, M. Chen, M. Zamani, M. Chern, P. Aquino, X. Zhang, S. Lecommandoux, A. Fan, M. Cabodi, C. Klapperich, M. W. Grinstaff, A. M. Dennis, J. E. Galagan, *Nature Communications* **2020**, *11*, 1276.
[5] R. Bumgarner, *Current Protocols in Molecular Biology* **2013**, *101*, 22.1.1.
[6] Z. Lin, X. Li, H.-B. Kraatz, *Anal. Chem.* **2011**, *83*, 6896.
[7] A. A. Ensafi, B. Rezaei, M. Amini, E. Heydari-Bafrooei, *Talanta* **2012**, *88*, 244.
[8] a) I. Chopra, M. Roberts, *Microbiol Mol Biol Rev* **2001**, *65*, 232; b) M. O. Griffin, E. Fricovsky, G. Ceballos, F. Villarreal, *Am J Physiol Cell Physiol* **2010**, *299*, C539.
[9] R. J. Fair, Y. Tor, *Perspect Medicin Chem* **2014**, *6*, 25.
[10] M. Amjadi, J. L. Manzoori, F. Pakpoor, *Journal of Analytical Chemistry* **2016**, *71*, 253.
[11] a) S. Sczesny, H. Nau, G. Hamscher, *Journal of Agricultural and Food Chemistry* **2003**, *51*, 697; b) H. De Ruyck, H. De Ridder, *Rapid Commun. Mass Spectrom.* **2007**, *21*, 1511.
[12] a) N. Prado, E. Renault, J. Ochoa, A. Amrane, *Environmental Technology* **2009**, *30*, 469; b) J. Zhou, X. Xue, Y. Li, J. Zhang, F. Chen, L. Wu, L. Chen, J. Zhao, *Food Chemistry* **2009**, *115*, 1074.
[13] A. Siljanoski, R. Ciglarič, T. Pezdir, P. R. Lainšček, J. Dolenc, J. Starič, K. Šinigoj-Gačnik, *Journal of Dairy Research* **2018**, *85*, 321.
[14] X. P. Zhang, R. R. Zhang, A. J. Yang, Q. Wang, R. M. Kong, F. L. Qu, *Microchim. Acta* **2017**, *184*, 4367.
[15] X. Liu, T. Wang, W. Wang, Z. Zhou, Y. Yan, *Journal of Industrial and Engineering Chemistry* **2019**, *72*, 100.
[16] L. Cuthbertson, J. R. Nodwell, *Microbiology and Molecular Biology Reviews* **2013**, *77*, 440.
[17] N. D. Taylor, A. S. Garruss, R. Moretti, S. Chan, M. A. Arbing, D. Cascio, J. K. Rogers, F. J. Isaacs, S. Kosuri, D. Baker, S. Fields, G. M. Church, S. Raman, *Nature Methods* **2015**, *13*, 177.
[18] A. Sassolas, B. D. Leca-Bouvier, L. J. Blum, *Chemical Reviews* **2008**, *108*, 109.
[19] D.-S. Wang, S.-K. Fan, *Sensors* **2016**, *16*, 1175.
[20] T. Kamra, T. Zhou, L. Montelius, J. Schnadt, L. Ye, *Anal. Chem.* **2015**, *87*, 5056.
[21] M. Hegner, P. Wagner, G. Semenza, *FEBS Letters* **1993**, *336*, 452.
[22] X. Lv, L. Chen, H. Zhang, J. Mo, F. Zhong, C. Lv, J. Ma, Z. Jia, *Biosensors and Bioelectronics* **2013**, *39*, 329.
[23] a) A. A. Ensafi, E. Heydari-Bafrooei, M. Amini, *Biosensors and Bioelectronics* **2012**, *31*, 376; b) E. Dubuisson, Z. Yang, K. P. Loh, *Anal. Chem.* **2011**, *83*, 2452.
[24] W. R. Algar, U. J. Krull, *Langmuir* **2008**, *24*, 5514.

[25] M. Chern, T. T. Nguyen, A. H. Mahler, A. M. Dennis, *Nanoscale* **2017**, *9*, 16446.
[26] K. Susumu, E. Oh, J. B. Delehanty, J. B. Blanco-Canosa, B. J. Johnson, V. Jain, W. J. Hervey, W. R. Algar, K. Boeneman, P. E. Dawson, I. L. Medintz, *Journal of the American Chemical Society* **2011**, *133*, 9480.
[27] a) Y. Han, M. O. Noor, A. Sedighi, U. Uddayasankar, S. Doughan, U. J. Krull, *Langmuir* **2017**, *33*, 12839; b) M. La Rosa, T. Avellini, C. Lincheneau, S. Silvi, I. A. Wright, E. C. Constable, A. Credi, *European Journal of Inorganic Chemistry* **2017**, *2017*, 5143.
[28] a) E. R. Goldman, I. L. Medintz, A. Hayhurst, G. P. Anderson, J. M. Mauro, B. L. Iverson, G. Georgiou, H. Mattoussi, *Anal. Chim. Acta* **2005**, *534*, 63; b) K. E. Sapsford, T. Pons, I. L. Medintz, S. Higashiya, F. M. Brunel, P. E. Dawson, H. Mattoussi, *The Journal of Physical Chemistry C* **2007**, *111*, 11528; c) T. T. Nguyen, M. Chern, R. C. Baer, J. Galagan, A. M. Dennis, *Small* **2020**, *16*, 1907522.
[29] T. M. Herne, M. J. Tarlov, *Journal of the American Chemical Society* **1997**, *119*, 8916.
[30] a) A. M. Wagner, J. M. Knipe, G. Orive, N. A. Peppas, *Acta Biomaterialia* **2019**; b) A. Shahmuradyan, M. Moazami-Goudarzi, F. Kitazume, G. S. Espie, U. J. Krull, *Analyst* **2019**, *144*, 1223; c) B. Wang, Z. You, D. H. Ren, *Analyst* **2019**, *144*, 2304; d) A. Lesiak, K. Drzozga, J. Cabaj, M. Banski, K. Malecha, A. Podhorodecki, *Nanomaterials* **2019**, *9*, 24; e) S. Jung, X. Y. Chen, *Adv. Healthc. Mater.* **2018**, *7*, 14.
[31] U. Uddayasankar, U. J. Krull, *Langmuir* **2015**, *31*, 8194.
[32] W. R. Algar, U. J. Krull, *Langmuir* **2009**, *25*, 633.
[33] C. E. Immoos, S. J. Lee, M. W. Grinstaff, *Chembiochem* **2004**, *5*, 1100.
[34] J. G. Forbes, A. J. Jin, K. Wang, *Langmuir* **2001**, *17*, 3067.
[35] H.-J. Butt, B. Cappella, M. Kappl, *Surface Science Reports* **2005**, *59*, 1.
[36] P. Orth, D. Schnappinger, W. Hillen, W. Saenger, W. Hinrichs, *Nat Struct Biol* **2000**, *7*, 215.
[37] R. Fernandez-Lopez, R. Ruiz, F. de la Cruz, G. Moncalian, *Front Microbiol* **2015**, *6*, 648.
[38] R. Fernandez-López, R. Ruiz, F. de la Cruz, G. Moncalián, *Frontiers in Microbiology* **2015**, *6*.
[39] M. B. Keeley, J. Busch, R. Singh, T. Abel, *BioTechniques* **2005**, *39*, 529.
[40] a) O. Scholz, M. Köstner, M. Reich, S. Gastiger, W. Hillen, *Journal of Molecular Biology* **2003**, *329*, 217; b) E.-M. Henssler, O. Scholz, S. Lochner, P. Gmeiner, W. Hillen, *Biochemistry* **2004**, *43*, 9512.
[41] C. Daniel, Y. Roupioz, D. Gasparutto, T. Livache, A. Buhot, *PLOS ONE* **2013**, *8*, e75419.
[42] S. Li, L. Zhou, Y. Yao, K. Fan, Z. Li, L. Zhang, W. Wang, K. Yang, *Chemical Communications* **2017**, *53*, 99.
[43] K. K. Alam, J. K. Jung, M. S. Verosloff, P. R. Clauer, J. W. Lee, D. A. Capdevila, P. A. Pastén, D. P. Giedroc, J. J. Collins, J. B. Lucks, *bioRxiv* **2019**, 619296.
[44] Y. Yao, S. Li, J. Cao, W. Liu, K. Fan, W. Xiang, K. Yang, D. Kong, W. Wang, *Chemical Communications* **2018**, *54*, 4774.
[45] M. Liang, Z. Li, W. Wang, J. Liu, L. Liu, G. Zhu, L. Karthik, M. Wang, K.-F. Wang, Z. Wang, J. Yu, Y. Shuai, J. Yu, L. Zhang, Z. Yang, C. Li, Q. Zhang, T. Shi, L. Zhou, F. Xie, H. Dai, X. Liu, J. Zhang, G. Liu, Y. Zhuo, B. Zhang, C. Liu, S. Li, X. Xia, Y. Tong, Y. Liu, G. Alterovitz, G.-Y. Tan, L.-X. Zhang, *Nature Communications* **2019**, *10*, 3672.
[46] a) S. Vigneshvar, C. C. Sudhakumari, B. Senthilkumaran, H. Prakash, *Front. Bioeng. Biotechnol.* **2016**, *4*, 9; b) M. O. Noor, E. Petryayeva, A. J. Tavares, U.

Uddayasankar, W. R. Algar, U. J. Krull, *Coordination Chemistry Reviews* **2014**, *263–264*, 25.
[47] M. Franke, S. Leubner, A. Dubavik, A. George, T. Savchenko, C. Pini, P. Frank, D. Melnikau, Y. Rakovich, N. Gaponik, A. Eychmuller, A. Richter, *Nanoscale Res. Lett.* **2017**, *12*, 8.
[48] W. R. Algar, U. J. Krull, *Anal. Chem.* **2009**, *81*, 4113.
[49] K. Pardee, A. A. Green, T. Ferrante, D. E. Cameron, A. DaleyKeyser, P. Yin, J. J. Collins, *Cell* **2014**, *159*, 940.
[50] Y. Yao, S. Li, J. Cao, W. Liu, F. Qi, W. Xiang, K. Yang, W. Wang, L. Zhang, *Appl. Microbiol. Biotechnol.* **2018**, *102*, 7489.
[51] Y. Ghosh, B. D. Mangum, J. L. Casson, D. J. Williams, H. Htoon, J. A. Hollingsworth, *Journal of the American Chemical Society* **2012**, *134*, 9634.
[52] X. Li, D. Shen, J. Yang, C. Yao, R. Che, F. Zhang, D. Zhao, *Chemistry of Materials* **2013**, *25*, 106.
[53] K. Susumu, E. Oh, J. B. Delehanty, J. B. Blanco-Canosa, B. J. Johnson, V. Jain, W. J. t. Hervey, W. R. Algar, K. Boeneman, P. E. Dawson, I. L. Medintz, *J Am Chem Soc* **2011**, *133*, 9480.
[54] Time-Domain Lifetime Measurements. In *Principles of Fluorescence Spectroscopy*, Lakowicz, J. R., Ed. Springer US: Boston, MA, 2006; pp 97.
[55] L. M. Demers, C. A. Mirkin, R. C. Mucic, R. A. Reynolds, R. L. Letsinger, R. Elghanian, G. Viswanadham, *Anal. Chem.* **2000**, *72*, 5535.
[56] A. B. Steel, T. M. Herne, M. J. Tarlov, *Anal. Chem.* **1998**, *70*, 4670.
[57] J. L. Sebaugh, P. D. McCray, *Pharmaceutical Statistics* **2003**, *2*, 167.

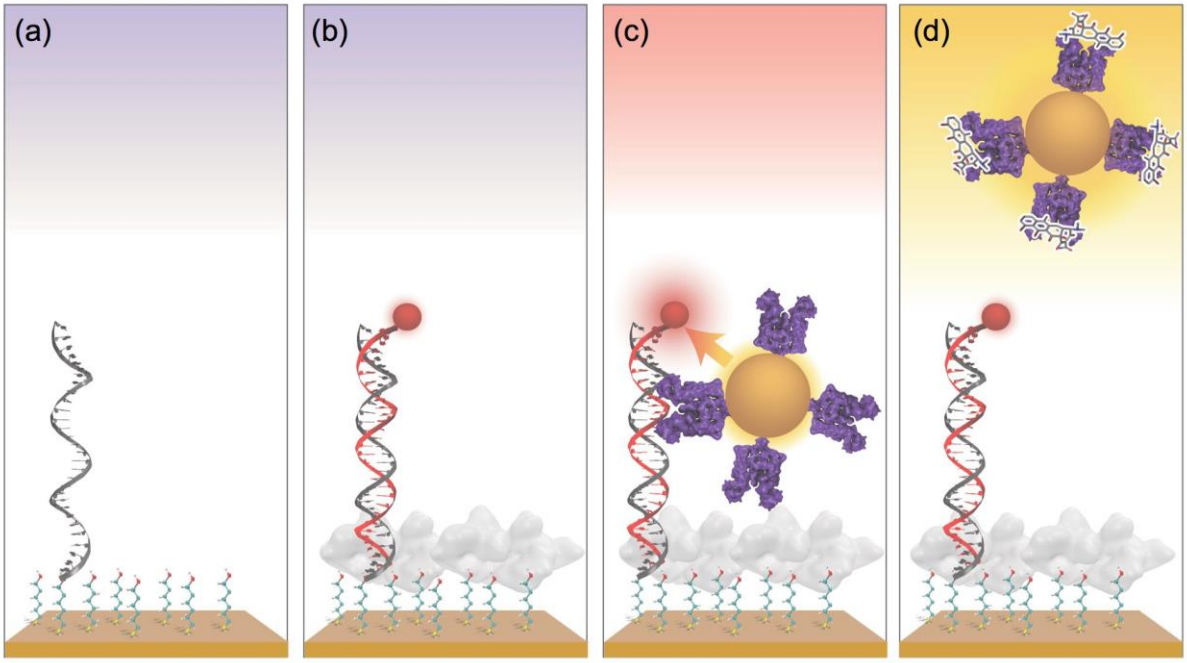

Figure 1. Preparation of probe system on gold surface, and its mechanism of action (not to scale). (a) Oligonucleotides (DNA) are immobilized to the gold surface (Au) with mercaptohexanol (MCH) as filler. (b) A fluorophore-labeled complementary DNA strand (Cy5-DNA) is hybridized to the immobilized oligonucleotide before bovine serum albumin (BSA) is added as a passivation layer. (c) Transcription factor TetR - quantum dot conjugates (TetR-QD) bind to their immobilized cognate DNA sequence, resulting in the fully assembled sensor. FRET occurs between QD and Cy5 as noted by the arrow. (d) Upon anhydrotetracycline addition, detection is recorded as a loss of signal (i.e., off-sensor).

M. Chen,T. T. Nguyen, N. Varongchayakul, C. Grazon, M. Chern, R C. Baer, S. Lecommandoux, C. M. Klapperich, J. E. Galagan, A. M. Dennis, M.W. Grinstaff Adv. Healthcare Mater. 2020 doi.org/10.1002/adhm.202000403

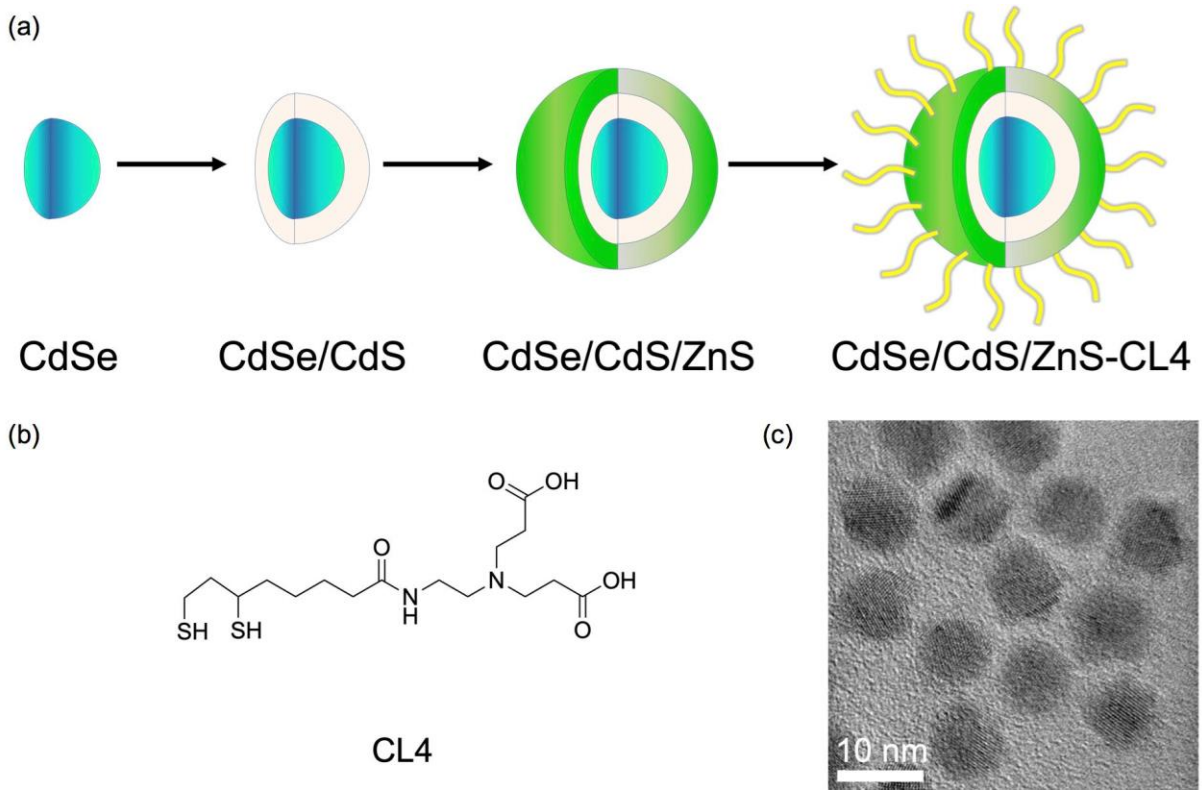

Figure 2. QD preparation and characterization. (a) Synthesis was performed using a successive ion layer adsorption and reaction (SILAR) method. QDs were subsequently functionalized with compact ligand (CL4) to render water solubility.[26] (b) TEM of QDs.

M. Chen,T. T. Nguyen, N. Varongchayakul, C. Grazon, M. Chern, R C. Baer, S. Lecommandoux, C. M. Klapperich, J. E. Galagan, A. M. Dennis, M.W. Grinstaff Adv. Healthcare Mater. 2020 doi.org/10.1002/adhm.202000403

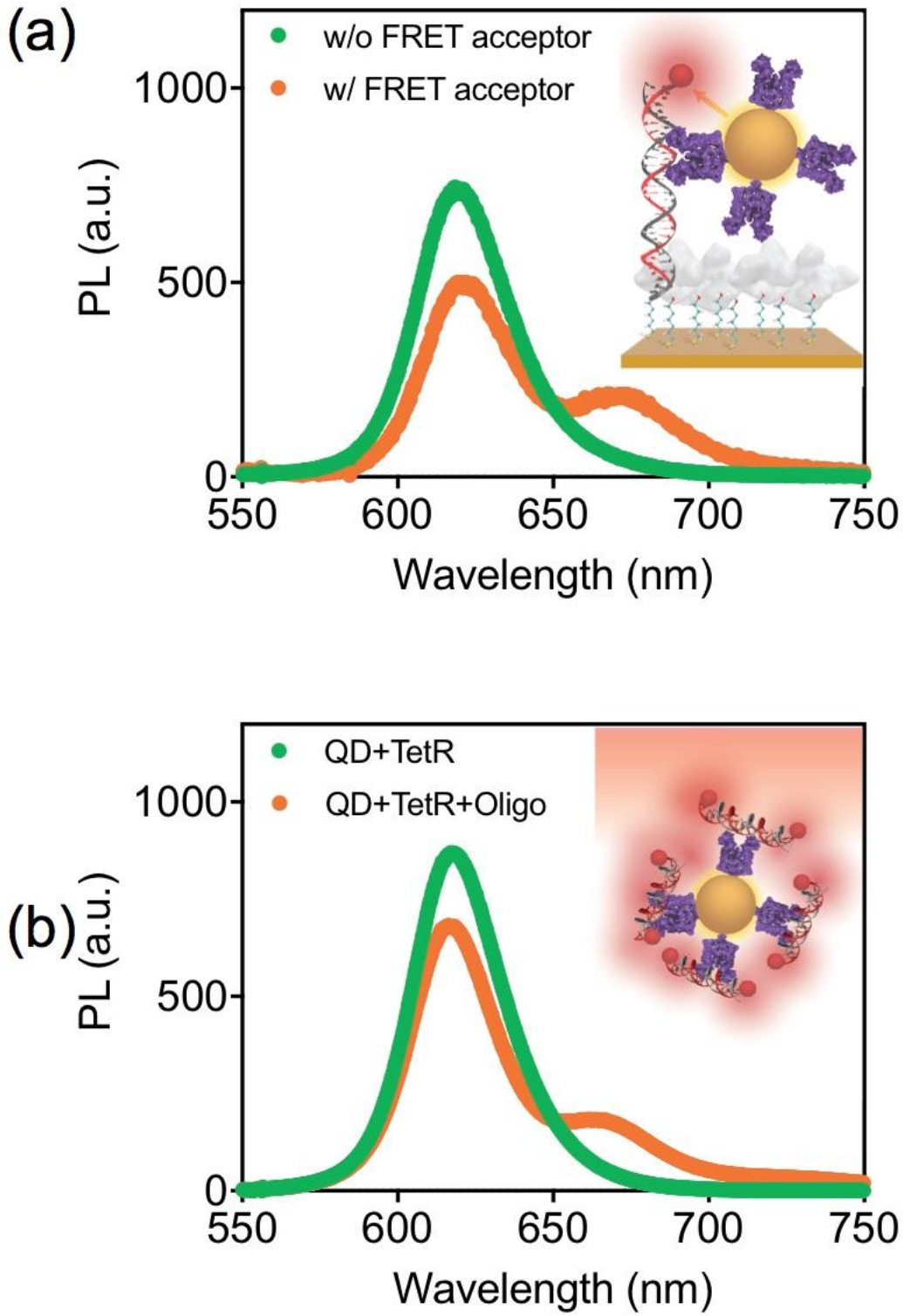

Figure 3. Photoluminescence spectra of surface probe system compared to the solution-phase QD-FRET system (λ_{exc}= 400 nm). (a) Spectra of immobilized surface probe system Au/MCH/Cy5-DNA/BSA + (TetR-QD) with FRET acceptor and Au/MCH/DNA/BSA + (TetR-QD) without FRET acceptor. (b) In solution, spectra with FRET: (Cy5-DNA) + (TetR-QD), and without FRET: (TetR-QD).

M. Chen,T. T. Nguyen, N. Varongchayakul, C. Grazon, M. Chern, R C. Baer, S. Lecommandoux, C. M. Klapperich, J. E. Galagan, A. M. Dennis, M.W. Grinstaff Adv. Healthcare Mater. 2020 doi.org/10.1002/adhm.202000403

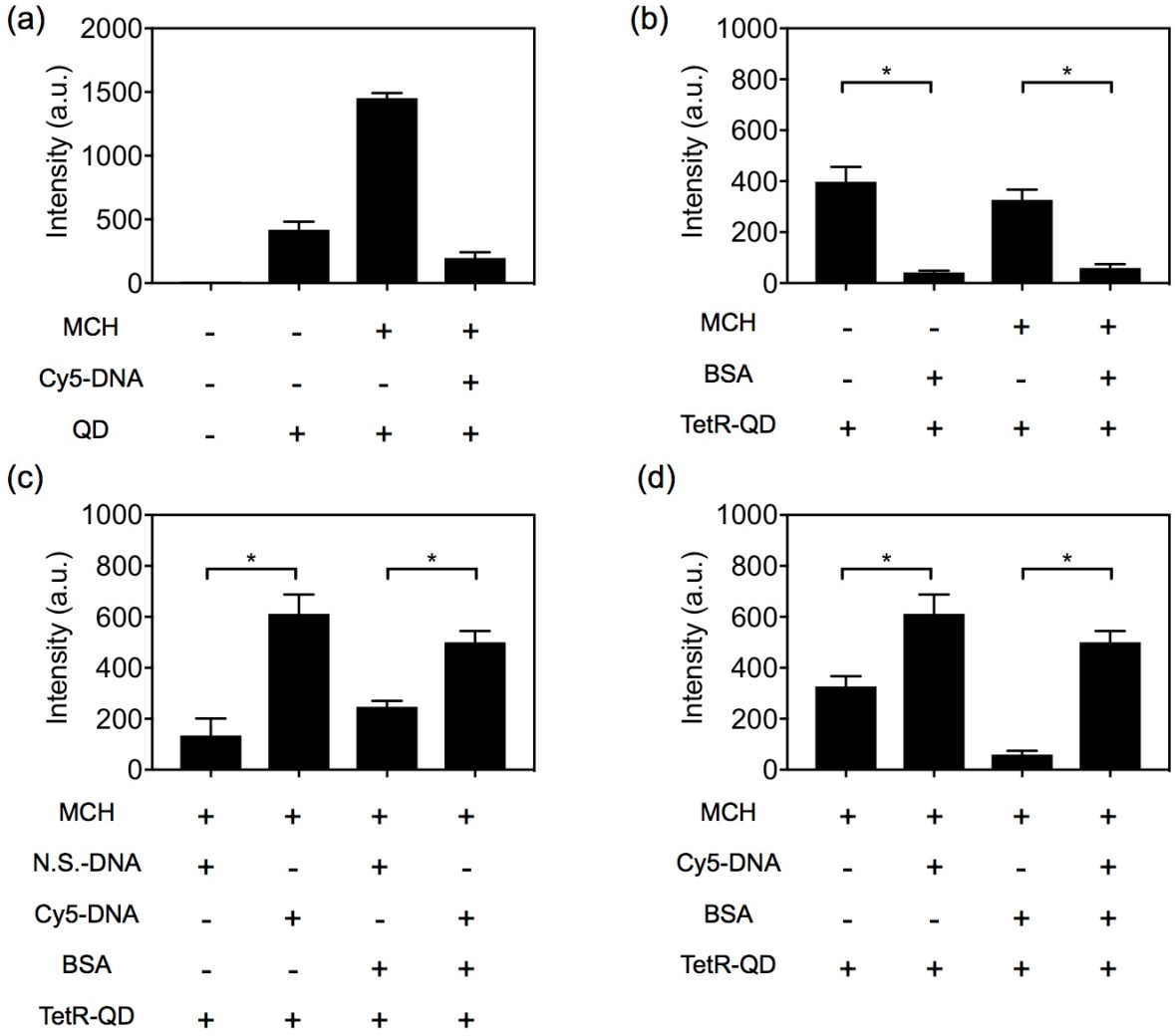

Figure 4. Fluorescence intensities of QD, QD-TF at 620 nm bound to the surface. (a) nonspecific adsorption of QD to various surfaces. (b) effect of BSA on nonspecific adsorption. (c) effect of DNA sequence (nonspecific vs specific). (d) effect of operator DNA (with vs without). Quantum dots, and transcription factor TetR - quantum dot conjugates binding to various surfaces after 10 min treatment. Intensity is measured when excited at 400 nm. Respective surfaces are named by their modifier content. For example, hybridizing transcription factor recognizing sequence of oligonucleotides with Cy5-labled complementary strand Cy5-DNA, with mercaptohexanol as filler and BSA as passivation layer, followed by TetR-QD attachment to the surface yields the preparation of surface 'Au/MCH/Cy5-DNA/BSA + (TetR-QD)'. 'N.S.-DNA' represents the nonspecific sequence of oligonucleotide variant. Error bars of intensity measurement represent standard deviation values, n=3. Multivariance analysis was done using one-way ANOVA that was corrected using the Bartlett's variance test, and for multiple comparisons, the Bonferroni multiple-comparison test was used. *Statistical significance (95% confidence) for samples with and without BSA, and transcription factor recognizing sequence of oligonucleotides.

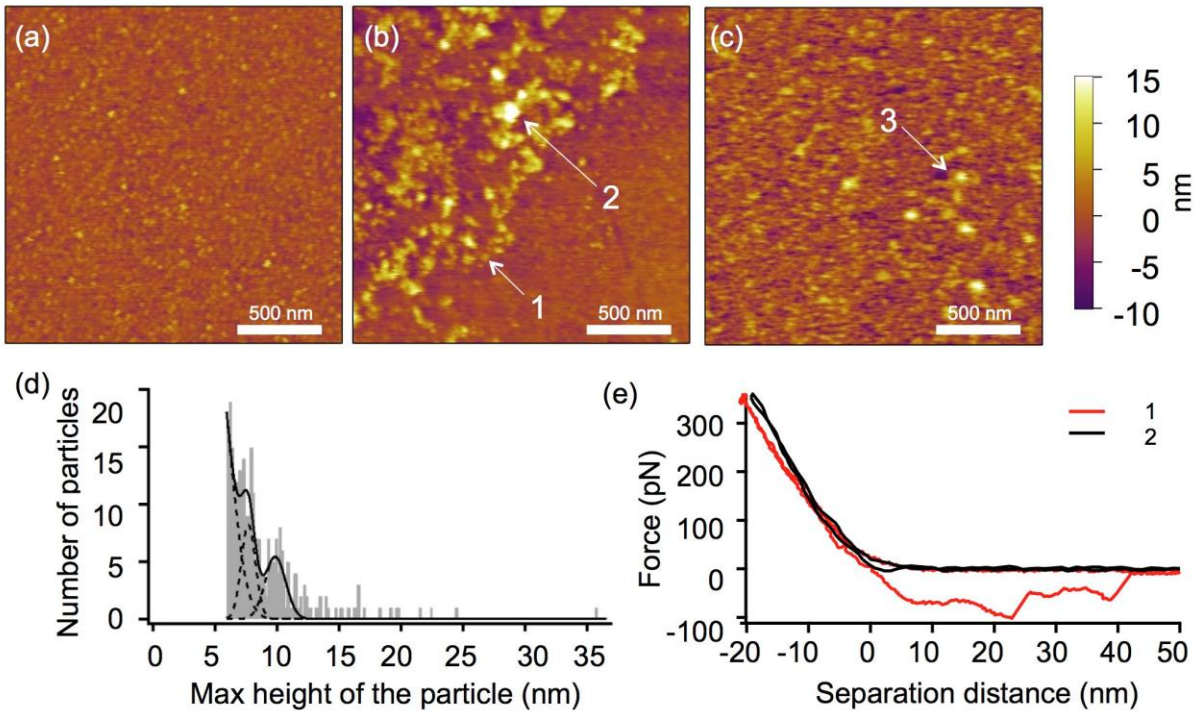

Figure 5. AFM images depicting the topography and roughness of surface, and identification of the species. (a) the surface with DNA and filler, Au/MCH/Cy5-DNA, roughness = 1.5 nm, (b) assembled surface probe system before aTc addition, Au/MCH/Cy5-DNA/BSA +(TetR-QD), roughness = 3.2 nm, (c) surface probe system after aTc addition, roughness = 1.7 nm, (d) histogram of the particle size on the surface of Au/MCH/Cy5-DNA/BSA +(TetR-QD). The masking process renders a particle size cutoff at 6 nm. Fitting with multi-Gaussian function yields peaks at 7.7 ± 0.8 nm and 9.9 ± 1.2 nm (marked as spot 1 and spot 3, respectively). Additional population of the particles with height greater than 15.0 nm is marked as spot 2. (e) Representative force spectra, both approaching and retracting curves from spot 1 (red), and spot 2 (black). Spots 1 and 2 likely represent BSA and QD- TF conjugate, respectively.

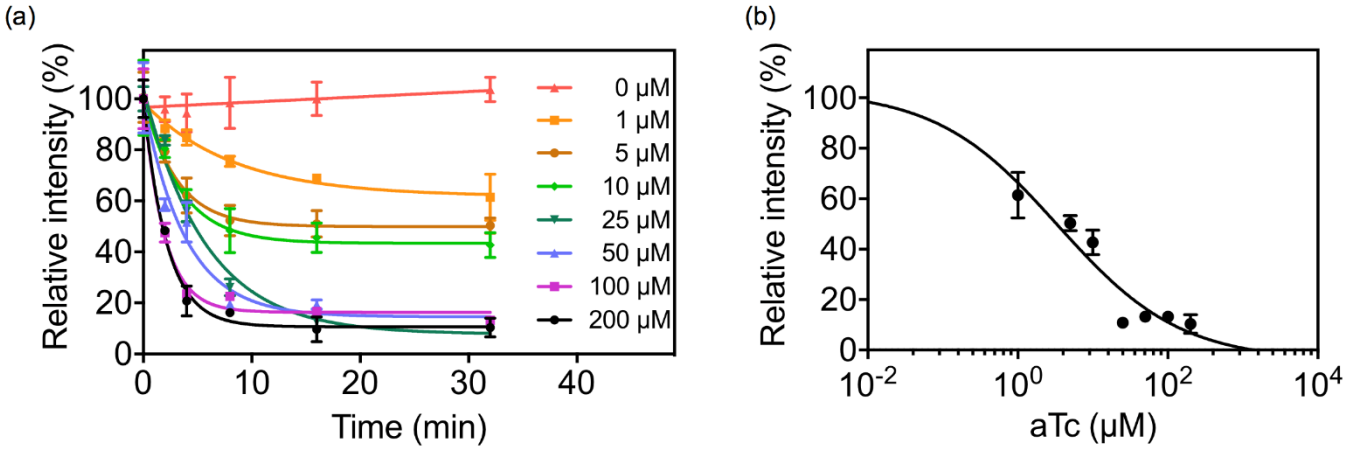

Figure 6. Dose response of surface probe system. (a) Dose responses of Au/MCH/Cy5-DNA/BSA +(TetR-QD) surface are compared among various concentrations of aTc over time. Emission intensity at 620 nm was measured in relative fluorescence units (RFU), reported relative to initial intensity (t=0). (b) Effect of aTc concentration on surface probe system response. Relative intensity (t=32 min) data is presented as representative experiments measured by spectrofluorometer and reported by percentage of QD emission intensity on the sample surfaces. Error bars denote standard deviations, n=3.

Supporting Information

Table S1. Oligonucleotide sequences

#	Function	Sequence	After hybridization
1	Cognate DNA, binds to Au surface	SH-C6-TCA GTA TCT CTA TCA ATG ATA GGG ATG ACT	1 and 2 form cognate DNA labeled with Cy5
2	complementary to 1, with Cy5 at its end	Cy5-AGT CAT CCC TAT CAT TGA TAG AGA TAC TGA	
3	complementary to 1, without Cy5 at its end	AGT CAT CCC TAT CAT TGA TAG AGA TAC TGA	1 and 3 form cognate DNA
4	scrambled DNA, binds to Au surface	SH-C6-ACA CGC ACA GGG AGC GAG CCA AAG TGC T	4 and 5 form non-specific DNA control sequence
5	complementary to 4	Cy5-AGC ACT TTG GCT CGC TCC CTG TGC GTG T	
6	cognate DNA, does not bind to Au	Cy5-CA GTA TCT CTA TCA ATG ATA GGG ATG AC-Cy5	6 and 7 form solution-phase Cy5-labeled cognate DNA
7		GTC ATC CCT ATC ATT GAT AGA GAT ACT G	

Table S2. Surface probe system responses at different time points.

Time [min]	IC_{50} [μM]	R square	Hill Slope	LOD [μM]	Linear range [μM]
2	398	0.87	-0.50	1.5	19 to 8510
4	91	0.96	-0.50	0.23	4 to 2001
8	4.7	0.96	-0.73	0.3	1 to 38
16	4.3	0.95	-0.65	0.15	0.4 to 47
32	3.4	0.95	-0.53	0.08	0.19 to 62

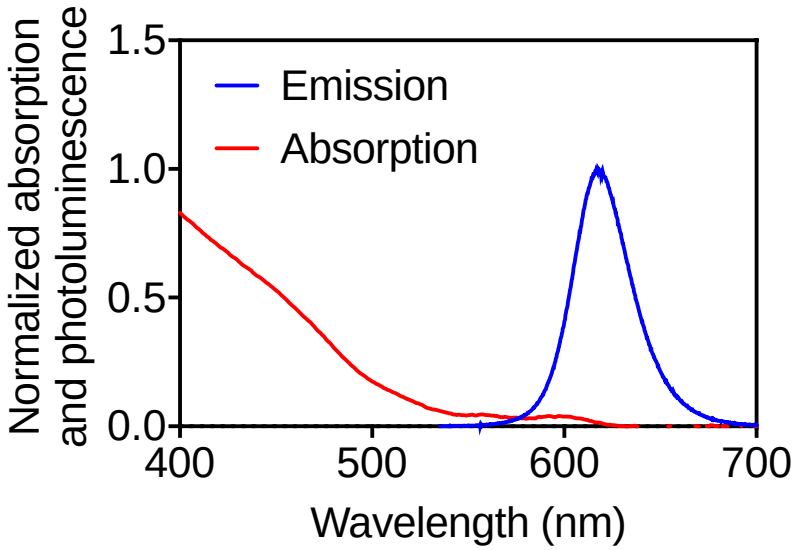

Figure S1. QD absorption and emission (λ_{exc}= 400 nm) spectra in PBS.

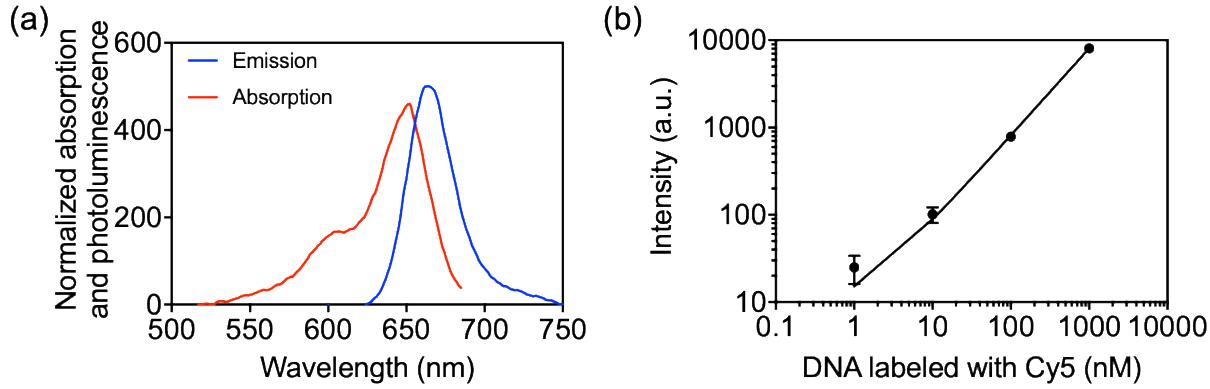

Figure S2. (a) Cy5-DNA absorption and emission (λ_{exc}= 590 nm) spectra in PBS. (b) Cy5 emission intensity vs DNA labeled with Cy5 concentration standard curve. Error bars denote standard deviations, n=3.

M. Chen,T. T. Nguyen, N. Varongchayakul, C. Grazon, M. Chern, R C. Baer, S. Lecommandoux, C. M. Klapperich, J. E. Galagan, A. M. Dennis, M.W. Grinstaff Adv. Healthcare Mater. 2020 doi.org/10.1002/adhm.202000403

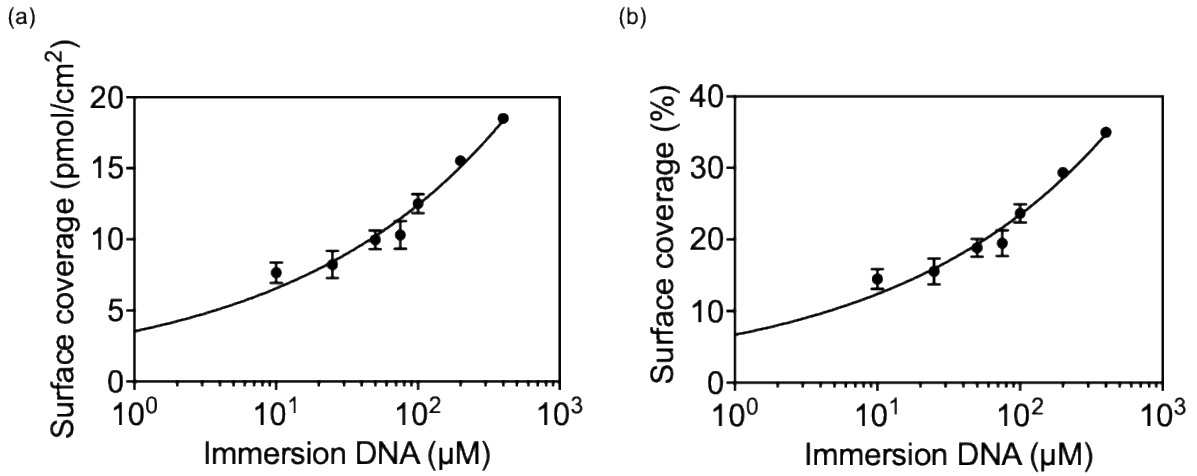

Figure S3. Correlation of the DNA surface density and applied DNA concentration. (a) DNA surface density was measured by detecting dehybridized complementary strand labeled with fluorophore. (b) DNA surface coverage. Error bars denote standard deviations, n=3.

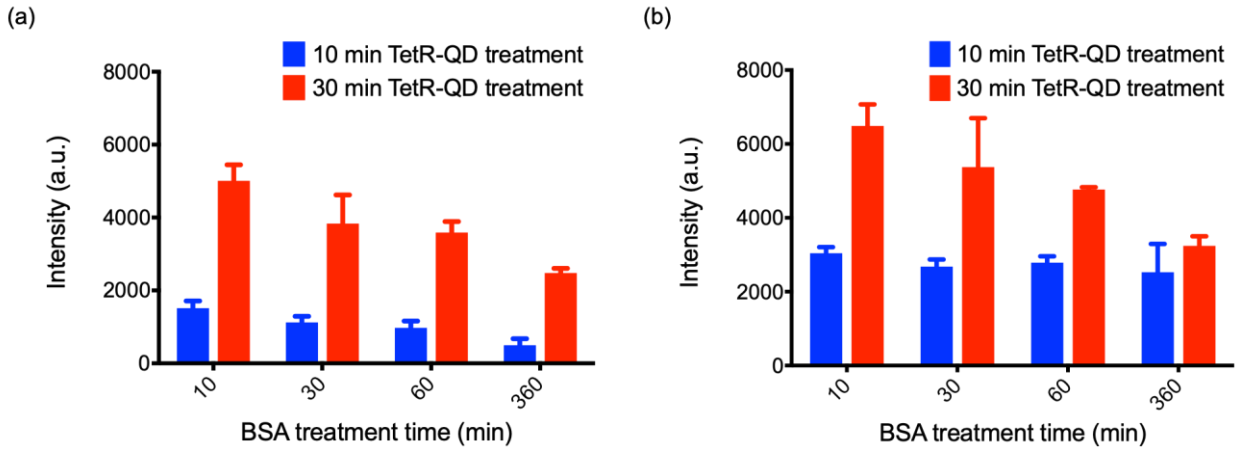

Figure S4. Effect of BSA concentration, BSA treatment time, (TetR-QD) incubation time on binding to surface. Intensity is measured at 620 nm in relative fluorescence units, when excited at 400 nm. With 0.05% (a) and 0.5% (b) BSA to form passivation layer, the relative QD emission intensity after TetR-QD treatment. Intensity of emission at 620 nm is used as an indicator of amount of QD-TF bound to the surface. Error bars denote standard deviations, n=3.

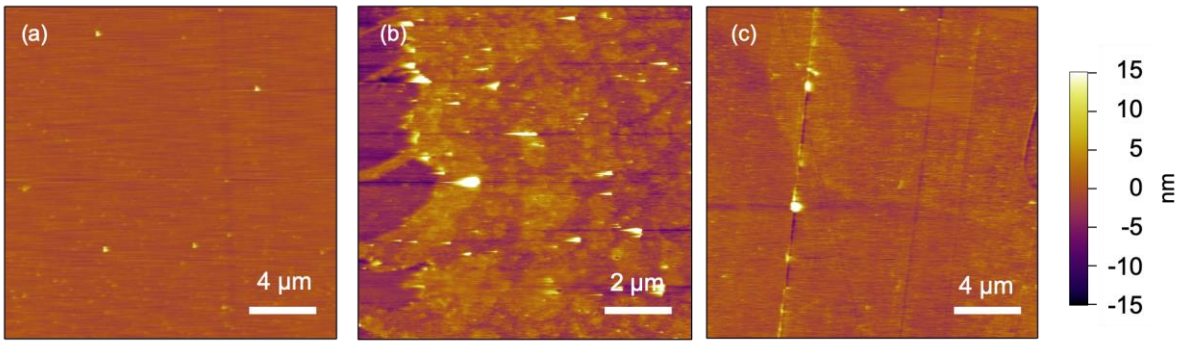

Figure S5. 2D AFM images depicting the topography of surface. (a) the surface with DNA and filler, Au/MCH/Cy5-DNA. (b) assembled surface probe system before aTc addition, Au/MCH/Cy5-DNA/BSA +(TetR-QD). (c) the surface probe system after aTc addition.

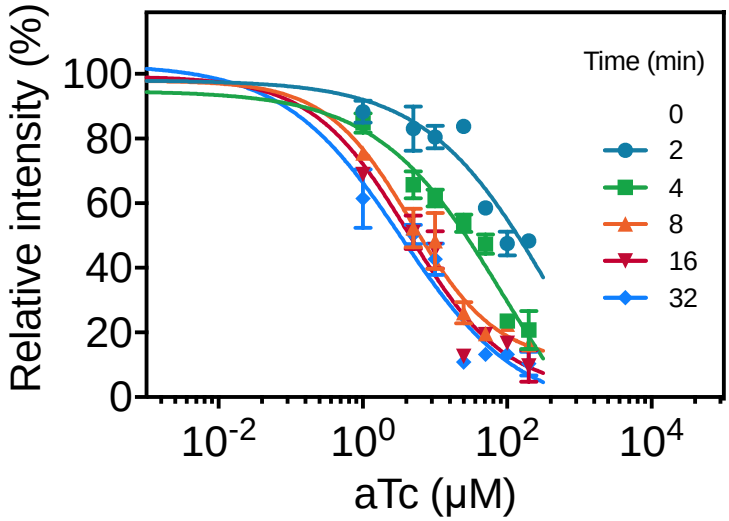

Figure S6. Effect of aTc concentration on surface probe system response at different time points. Relative intensity data was measured with a spectrofluorometer and reported as a percentage of QD emission intensity on the sample surfaces. Error bars denote standard deviations, n=3.